ACS APPLIED MATERIALS & INTERFACES

LETTER

www.acsami.org

Solution-Processed MoO_3 Thin Films As a Hole-Injection Layer for Organic Solar Cells

Claudio Girotto,[†,⊥] Eszter Voroshazi,[†,‡] David Cheyns,[†] Paul Heremans,[†,‡] and Barry P. Rand[*,†]

[†]imec, Kapeldreef 75, 3001 Leuven, Belgium

[‡]ESAT, Katholieke Universiteit Leuven, Kasteelpark Arenberg 10, 3001 Leuven, Belgium

Supporting Information

ABSTRACT: We report on a sol−gel-based technique to fabricate MoO_3 thin films as a hole-injection layer for solution-processed or thermally evaporated organic solar cells. The solution-processed MoO_3 ($sMoO_3$) films are demonstrated to have equal performance to hole-injection layers composed of either PEDOT:PSS or thermally evaporated MoO_3 ($eMoO_3$), and the annealing temperature at which the sol−gel layer begins to work is consistent with the thermodynamic analysis of the process. Finally, the shelf lifetime of devices made with the $sMoO_3$ is similar to equivalent devices prepared with a $eMoO_3$ hole-injection layer.

KEYWORDS: hole-injection layer, solution processing, sol−gel technique, molybdenum oxide, organic solar cells

Organic solar cells show great potential as a low-cost and lightweight energy source, and their certified efficiency recently reached values above 8%.[1] Among these cells, polymer based devices are attractive as they can be deposited from solution in roll-to-roll systems, benefiting from the high manufacturability of this method[2−4]

The typical organic solar cell device structure includes a transparent electrode based on indium tin oxide (ITO) and a hole-injection layer (HIL) to reduce roughness and/or obtain an efficient hole-extraction from the organic materials with deep highest occupied molecular orbital (HOMO) levels in the active layer.[5]

Poly(3,4-ethylenedioxythiophene):poly(styrenesulfonate) (PEDOT:PSS) is often used as HIL because of its easy processability, smooth surface, and the match of its work function to the HOMO level of many donor-type organic semiconductors. Recent studies revealed that the intrinsic device stability in ambient conditions for devices incorporating PEDOT:PSS is compromised by its hygroscopic nature, which introduces humidity in the devices and degrades the low-work-function metal.[6,7]

Transition metal oxides, such as MoO_3, V_2O_5, NiO, and WO_3,[8−11] have been employed as alternatives to PEDOT:PSS, based on the favorable energy level alignment[12] and the increased stability demonstrated in organic solar cells.[6] They can be deposited via various methods, including thermal or electron beam evaporation, sputtering,[10] or pulsed-laser deposition.[13] Alternatively, solution-processing methods have been demonstrated with the application from colloidal V_2O_5[14] or MoO_3 nanoparticle dispersions,[5,15] via the oxidation of a metalorganic Ni ink,[16] from combustion processing of diverse metal oxide[17] and, recently, with the sol−gel process of V_2O_5.[18] The latter method allows for precise composition control and high homogeneity, and is favorable for the application on large areas when low processing cost is preferred. We propose here a sol−gel process for MoO_3 as HIL for both polymer and small molecule based solar cells: we investigate the process as a function of temperature and compare the photovoltaic results and their stability with the ones obtained on analogous organic solar cells processed on PEDOT:PSS and evaporated MoO_3.

We developed the solution-processed MoO_3 ($sMoO_3$) HIL with the sol−gel technique by adapting the recipe proposed by Lin et al.:[19] 1 M solution of MoO_3 powder (99.5%, Sigma-Aldrich) in H_2O_2 (30%, Sigma-Aldrich) was refluxed for 2 h at 80 °C in air and then cooled to room temperature (RT) for 24 h to obtain a clear yellow liquid. The viscosity and concentration of the solution were further adjusted with the addition of polyethylene glycol (average M_n 400, Sigma-Aldrich) and 2-methoxyethanol (Sigma-Aldrich) under reflux (0.5 h at 70 °C and 60 °C, respectively, followed by 24 h at RT) with a volume ratio of 1:0.25:6.25. The bright yellow solution is stable over several days when an excess of H_2O_2 is present, whereas it changes into a dark blue solution when the H_2O_2 amount is not sufficient for the full conversion of MoO_3 into $MoO_2(OH)(OOH)$.[20]

The prepared yellow solution was spin-coated in air on ITO substrates (20 Ω/*sq*, Kintec), previously cleaned with a sequence of detergent, deionized water, acetone, and isopropanol in an ultrasonic bath, followed by ultraviolet/O_3 treatment. The samples were annealed for 10 min on a hot plate at temperatures from 100 °C to 350 °C in N_2. Film thicknesses were measured by ellipsometry measurements (GES5 from SOPRA).

Reference devices were produced on identical substrates either by thermally evaporating 20 nm of MoO_3 ($eMoO_3$) from the same initial powder (vacuum pressure 10^{-7} Torr) or by spin coating 30 nm of PEDOT:PSS (Baytron Clevios AI4083, H.C. Starck GmbH). For the production of polymer based solar cells, 220 nm of a mixture of poly-3(hexylthiophene) (P3HT, Rieke #4002-EE from Rieke Metals, Inc.) and (6,6)-phenyl C61-butyric acid methyl ester (PCBM, Solenne bv) dissolved in 1:1 weight ratio in ortho-dichlorobenzene (Sigma-Aldrich) at 25 mg/mL

Received: June 6, 2011
Accepted: August 10, 2011
Published: August 10, 2011

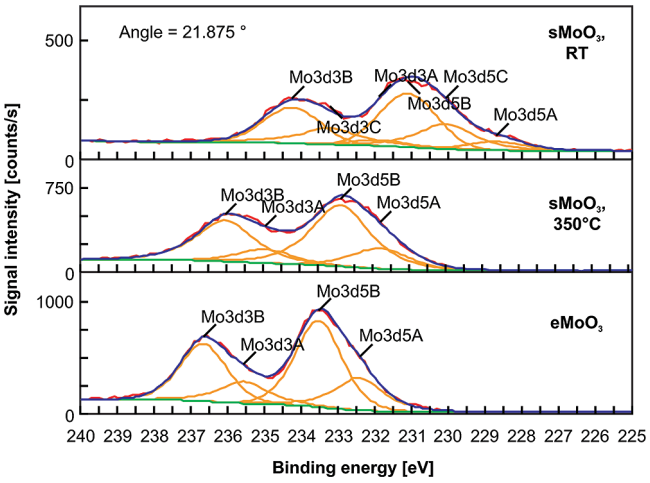

Figure 1. XPS spectra and deconvolutions of various MoO_3 layers.

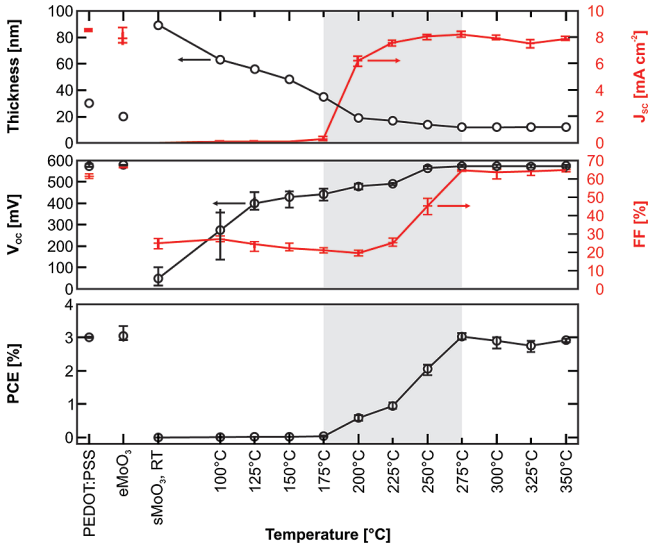

Figure 2. Thickness, short circuit current (J_{SC}), open circuit voltage (V_{OC}), fill factor (FF), and power conversion efficiency (PCE) of P3HT:PCBM-based solar cells processed on PEDOT:PSS, $eMoO_3$, and $sMoO_3$ treated at different temperatures.

were spin coated in N_2 adopting the slow drying method.[21] The cathode, composed by 40 nm Ca followed by 100 nm Ag, was thermally evaporated (base pressure 10^{-7} Torr) through a shadow mask to define active areas of 3 mm^2. Alternatively, small molecule based solar cells were produced by sequentially depositing 16 nm of chloroboron subphthalocyanine (SubPc, Aldrich), 35 nm of C_{60} (SES research), 10 nm of bathocuproine (Aldrich), all purified at least once using vacuum thermal gradient sublimation before loading them in a high-vacuum evaporation chamber (base pressure $<5 \times 10^{-7}$ Torr), followed by 150 nm Ag.

The current-density vs voltage ($J-V$) characterization was performed in a N_2 glovebox using a Keithley 2602A Source-Measure Unit and an Abet solar simulator with 100 mW cm^{-2} AM1.5G illumination, calibrated with an ISE Fraunhofer certified Si photodiode.

The X-ray photoelectron spectroscopy (XPS) measurements shown in Figure 1 were carried out in AR-mode using a Theta300 system from ThermoInstruments (monochromatized Al K_α X-ray source (1486.6 eV) and a spot size of 400 μm) on the solution processed samples before (RT) and after (350 °C) the thermal treatment and on the thermally evaporated reference sample. The 350 °C and the evaporated spectra, after alignment to the C1s reference, could be fitted with doublets, while the RT one was fitted with three peaks. In the RT sample, the Mo3d5A shoulder at 228.6 eV and the Mo3d5C peak around 230 eV can be ascribed to the metallic Mo and the Mo^{4+} peaks, respectively. In the 350 °C and evaporated samples, the Mo3d5B peak from Mo^{6+} can be found around 233 eV, confirming that the thermal treatment effectively contributes to the sol−gel conversion into MoO_3. Both the solution processed samples show broader Mo peaks and lower signal intensity as compared to the evaporated sample, suggesting the presence of several oxidation levels, characterized by a wider range of binding energies, and a lower concentration of Mo atoms in the solid film, diluted by the organic residue from the solvents in the film and by the presence of O and H atoms in the hydroperoxo complex.[19,20,22]

Atomic force microscopy scans (included in the Supporting Information) of MoO_3 films on glass reveals smooth surfaces both before and after the 350 °C thermal treatment, with peak to valley variations of 1.8 nm and surface root-mean-square roughness of 0.36 nm. The film after thermal treatment results uniform and compact and does not present pin-holes or porosity on the top surface. X-ray diffraction measurements (not included) do not show significant diffraction peaks, confirming the amorphous or nanocrystalline nature of the films at all the temperatures investigated, including the evaporated layer, the transition to the crystalline phase of MoO_3 being reported at temperatures above the ones used in this study.[19,20]

Figure 2 shows the trend of the photovoltaic response of devices processed on $sMoO_3$ layers and the thickness of the latter after annealing at different temperatures. At the upper end of this temperature range, the photovoltaic parameters and the final power conversion efficiency (PCE) reach values close to the PEDOT:PSS and $eMoO_3$ based samples, confirming the electrical suitability of the $sMoO_3$ film.

The decrease in thickness starts already after treatment at 100 °C, in agreement with the major weight loss derived from the thermal gravimetrical analysis (TGA) performed by Lin et al.,[19] ascribable to the elimination of absorbed water and solvents. We observed an increase in open circuit voltage (V_{OC}) already at the lowest annealing temperature, which saturates at temperatures above 250 °C. Then, there is an onset of short circuit current (J_{SC}) that starts at 175 °C and saturates at 225 °C. Finally, fill factor (FF) begins to increase at 250 °C and saturates above 275 °C . We suspect that V_{OC} begins to increase early on, once a built-in field is set up across the electrodes. Once the built-in field is strong enough, at short-circuit the photocurrent is extracted efficiently, and therefore J_{SC} increases rapidly. Finally, when the built-in field saturates, the FF, which represents how well carriers can be extracted at voltages near a flat band condition (i.e., at small built-in fields), is able to reach considerable values of 65%.

In our experience, the performance of thermally evaporated SubPc/C_{60} devices relies more critically than P3HT:PCBM ones on the properties of the HIL, as they present a wide range of values for V_{OC} and FF depending on the interface properties of the HIL layer, similar to other donor molecules with deep HOMO levels.[23] Therefore, these devices are a crucial indicator for the reliability of the $sMoO_3$ layers. The $J-V$ curves of these and of polymer based devices with the $sMoO_3$ HIL are compared to the analogous ones with the $eMoO_3$ HIL in Figure 3. Slight

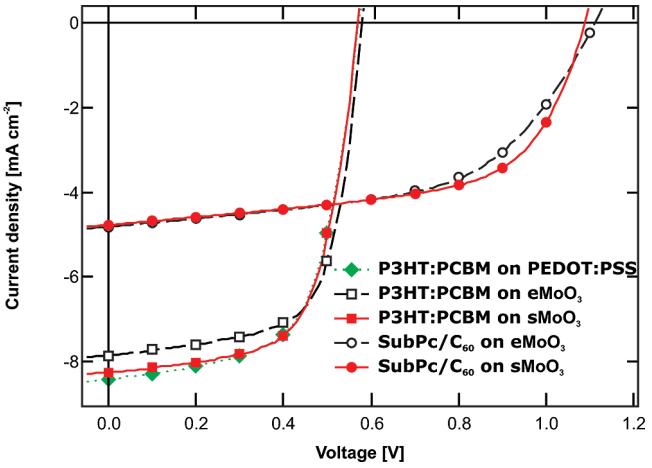

Figure 3. $J-V$ curves of P3HT:PCBM and SubPc/C_{60} organic solar cells processed on $sMoO_3$ and $eMoO_3$ hole-injection layers .

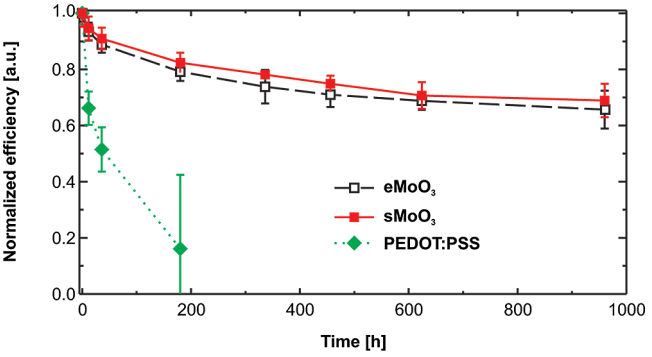

Figure 4. Normalized efficiency extracted from regular measurements of P3HT:PCBM-based devices stored in shelf life conditions.

variations in the performance of the devices confirm the strong similarity of the $sMoO_3$ with the $eMoO_3$: the P3HT:PCBM devices show a difference of only 0.4 mA cm^{-2} in J_{SC}, with changes in V_{OC} and FF within the error margin; the SubPc/C_{60} samples on $sMoO_3$ exhibit a sensibly higher FF than on $eMoO_3$, whereas J_{SC} and V_{OC} are not altered.

In Figure 4 the stability of devices based on the $sMoO_3$ with a cathode composed of 40 nm Yb and 100 nm Al is compared to devices based on $eMoO_3$ and on PEDOT:PSS in shelf life conditions (ISOS-D-1 Shelf[24]). PEDOT:PSS-based devices degrade to an average value below 20% of the initial efficiency within the first 200 h. In contrast, $sMoO_3$-based devices show remarkable stability, following the same trend as that of $eMoO_3$, with a PCE reducing to 70% of the initial values after 1000 h. The replacement of hygroscopic PEDOT:PSS with MoO_3 is effective in limiting the diffusion of humidity within the devices and thus in reducing the oxidation of the metals composing the cathode.[7]

In conclusion, we demonstrated a facile sol−gel-based technique to fabricate MoO_3 thin films as a hole-injection layer for solution-processed or thermally evaporated organic solar cells. The solution-processed MoO_3 films are demonstrated to have equal performance to hole-injection layers composed of either PEDOT or thermally evaporated MoO_3. From the evaluation of the electrical performance of layers, the thermal conversion of the precursor into MoO_3 is completed at temperatures around 275 °C, in agreement with the thermodynamic analysis of the reaction. Finally, the lifetime of devices made with the $sMoO_3$ in shelf life conditions are similar to equivalent devices made containing a $eMoO_3$ hole-injection layer, and outperform devices based on PEDOT:PSS.

■ ASSOCIATED CONTENT

Supporting Information. The atomic force microscopy scan of $sMoO_3$ film on glass after the thermal treatment (PDF). This material is available free of charge via the Internet at http://pubs.acs.org/.

■ AUTHOR INFORMATION

Corresponding Author

*E-mail: rand@imec.be.

Present Address

⊥Konarka Technologies, Inc., 116 John Street, Lowell, Massachusetts 01852, United States.

■ ACKNOWLEDGMENT

The authors thank Karolien Vasseur for the XRD measurements, Thierry Conard for the XPS measurements and Johan Wittevronghel for the preparation of the small molecule samples. The research was supported by the IWT SBO Project 06084 "PolySpec" funded by the Institute for the Promotion of Innovation by Science and Technology in Flanders (IWT).

■ REFERENCES

(1) Green, M. A.; Emery, K.; Hishikawa, Y.; Warta, W. *Prog. Photovoltaics: Res. Appl.* **2011**, *19*, 84–92.
(2) Girotto, C.; Rand, B. P.; Genoe, J.; Heremans, P. *Sol. Energy Mater. Sol. Cells* **2009**, *93*, 454–458.
(3) Girotto, C.; Rand, B. P.; Steudel, S.; Genoe, J.; Heremans, P. *Org. Electron* **2009**, *10*, 735–740.
(4) Girotto, C.; Moia, D.; Rand, B. P.; Heremans, P. *Adv. Funct. Mater.* **2011**, *21*, 64–2724.
(5) Meyer, J.; Khalandovsky, R.; Görrn, P.; Kahn, A. *Adv. Mater.* **2011**, *23*, 70–73.
(6) Voroshazi, E.; Verreet, B.; Aernouts, T.; Heremans, P. *Sol. Energy Mater. Sol. Cells* **2011**, *95*, 1303–1307.
(7) Voroshazi, E.; Verreet, B.; Buri, A.; Müller, R.; Di Nuzzo, D.; Heremans, P. *Org. Electron.* **2011**, *12*, 736–744.
(8) Chu, C.-W.; Li, S.-H.; Chen, C.-W.; Shrotriya, V.; Yang, Y. *Appl. Phys. Lett.* **2005**, *87*, 193508.
(9) Shrotriya, V.; Li, G.; Yao, Y.; Chu, C.-W.; Yang, Y. *Appl. Phys. Lett.* **2006**, *88*, 073508.
(10) Irwin, M. D.; Buchholz, D. B.; Hains, A. W.; Chang, R. P. H.; Marks, T. J. *Proc. Natl. Acad. Sci. U. S. A.* **2008**, *105*, 2783–2787.
(11) Tao, C.; Ruan, S.; Xie, G.; Kong, X.; Shen, L.; Meng, F.; Liu, C.; Zhang, X.; Dong, W.; Chen, W. *Appl. Phys. Lett.* **2009**, *94*, 043311.
(12) Tokito, S.; Noda, K.; Taga, Y. *J. Phys. D-Appl. Phys.* **1996**, *29*, 2750.
(13) Fan, X.; Fang, G.; Qin, P.; Sun, N.; Liu, N.; Zheng, Q.; Cheng, F.; Yuan, L.; Zhao, X. *J. Phys. D-Appl. Phys.* **2011**, *44*, 045101.
(14) Huang, J.-S.; Chou, C.-Y.; Liu, M.-Y.; Tsai, K.-H.; Lin, W.-H.; Lin, C.-F. *Org. Electron.* **2009**, *10*, 1060–1065.
(15) Liu, F.; Shao, S.; Guo, X.; Zhao, Y.; Xie, Z. *Sol. Energy Mater. Sol. Cells* **2010**, *94*, 842–845.
(16) Steirer, K. X.; Chesin, J. P.; Widjonarko, N. E.; Berry, J. J.; Miedaner, A.; Ginley, D. S.; Olson, D. C. *Org. Electron.* **2010**, *11*, 1414–1418.

(17) Kim, M.-G.; Kanatzidis, M. G.; Facchetti, A.; Marks, T. J. *Nat. Mater.* **2011**, *10*, 382–388.
(18) Zilberberg, K.; Trost, S.; Schmidt, H.; Riedl, T. *Adv. Energy Mater.* **2011**, *1*, 377–381.
(19) Lin, S.-Y.; Wang, C.-M.; Kao, K.-S.; Chen, Y.-C.; Liu, C.-C. *J. Sol−Gel Sci. Technol.* **2010**, *53*, 51–58.
(20) Kurusu, Y. *Bull. Chem. Soc. Jpn.* **1981**, *54*, 293–294.
(21) Li, G.; Shrotriya, V.; Huang, J.; Yao, Y.; Moriarty, T.; Emery, K.; Yang, Y. *Nat. Mater.* **2005**, *4*, 864–868.
(22) Segawa, K.; Ooga, K.; Kurusu, Y. *Bull. Chem. Soc. Jpn.* **1984**, *57*, 2721–2724.
(23) Hancox, I.; Chauhan, K. V.; Sullivan, P.; Hatton, R. A.; Moshar, A.; Mulcahy, C. P. A.; Jones, T. S. *Energy Environ. Sci.* **2010**, *3*, 107–110.
(24) Reese, M. O.; Gevorgyan, S. A.; Jørgensen, M.; Bundgaard, E.; Kurtz, S. R.; Ginley, D. S.; Olson, D. C.; Lloyd, M. T.; Morvillo, P.; Katz, E. A.; et al. *Sol. Energy Mater. Sol. Cells* **2011**, *95*, 1253–1267.